



Two years of Volatile Organic Compounds online in-situ measurements at SIRTA (Paris region, France) using Proton-Transfer-Reaction Mass Spectrometry

Leïla Simon^{1,2}, Valérie Gros¹, Jean-Eudes Petit¹, François Truong^{1,*}, Roland Sarda-Estève¹, Carmen Kalalian¹, Caroline Marchand², Olivier Favez²

¹Laboratoire des Sciences du Climat et de l'Environnement, Orme des Merisiers, 91190 Gif-sur-Yvette, France

²Institut National de l'Environnement Industriel et des Risques, Parc Technologique ALATA, 60550 Verneuil-en-Halatte, France

*Now at: Laboratoire Rhéologie et Procédés, 38610 Gières, France

Correspondence to: Valérie Gros (valerie.gros@lsce.ipsl.fr)

Abstract. Volatile Organic Compounds (VOCs) have direct influences on air quality and climate. They indeed play a key role in atmospheric chemistry, as precursors of secondary pollutants, such as ozone (O₃) and secondary organic aerosols (SOA). To this respect, long-term datasets of in-situ atmospheric measurements are crucial to characterize the variability of atmospheric chemical composition, its sources and trends. The on-going establishment of the Aerosols, Cloud, and Trace gases Research InfraStructure (ACTRIS) allows implementing the collection and provision of such high-quality datasets. In this context, online and continuous measurements of O₃, nitrogen oxides (NO_x) and aerosols have been carried out since 2012 at the SIRTA observatory, located in the Paris region, France. Within the last decade, VOC measurements have been conducted offline at SIRTA, until the implementation of a real-time monitoring which started in January 2020, using a Proton-Transfer-Reaction Quadrupole Mass-Spectrometer (PTR-Q-MS). The dataset acquired during the first two years of online VOC measurements provides insights on their seasonal and diurnal variabilities. The additional long-term datasets obtained from co-located measurements (NO_x, aerosol physical and chemical properties, meteorological parameters) are used to better characterize the atmospheric conditions and to further interpret the obtain results. Results also include insights on VOC's main sources and the influence of meteorological conditions and air mass origin on their levels, in the Paris region. Due to the COVID-19 pandemic, the year 2020 notably comprised a quasi-total lockdown in France in Spring, and a lighter one in Autumn. Therefore, a focus is made on the impact of these lockdowns on the VOC variability and sources. A change in the behaviour of VOC markers for anthropogenic sources was observed during the first lockdown, reflecting a change in human activities. This dataset could be further used as input for atmospheric models and can be found under <https://doi.org/10.14768/f8c46735-e6c3-45e2-8f6f-26c6d67c4723> (Simon et al, 2022).



1 Introduction

30 Long-term in situ measurements of atmospheric trace components are crucial to understand their variability, sources, processes, and long-term trends, influencing both air quality and climate (IPCC, 2021). To this end, the European Aerosol, Clouds, and Trace gases Research InfraStructure (ACTRIS, actris.eu) provides high quality data from in situ and remote sensing measurements. ACTRIS Topical Centers offer technical and scientific expertise such as guidelines and external quality assurance for the set-up of long-term measurements of short-lived atmospheric constituents. An important database containing
35 a large variety of datasets can be found on EBAS portal, including many variables at various European sites (actris.nilu.no). Among the components of interest within ACTRIS, Non-Methane Volatile Organic Compounds (NMVOCs, hereafter referred to as VOCs) are key pollutants, due to their multiple sources and high reactivity in the atmosphere (IPCC, 2021), acting as precursors for Secondary Organic Aerosols (SOA) and Ozone (O_3) in the troposphere. While atmospheric aerosols have direct and indirect impacts on the Earth radiative budget, O_3 acts as a greenhouse gas in the troposphere (IPCC, 2021). Additionally,
40 both are associated with adverse health effects (Daellenbach et al., 2020; Lefohn et al., 2018). To this respect, it is essential to characterize VOCs, their spatial and temporal variabilities as well as their sources, in order to best mitigate air pollution and minimize its impacts. While on a global scale, VOCs' main source is biogenic, anthropogenic sources such as traffic, residential wood burning and solvent use can have major contributions in urban areas, especially in winter (Baudic et al., 2016; Kaltsonoudis et al., 2016; Languille et al., 2020).

45 The Paris region is the most densely populated area in France with almost 20% of France's population in about 2% of the territory. The region comprises urban areas with city centres and substantial road traffic but also rural environments such as agricultural fields and forests, which represent both anthropogenic and natural sources of pollutants. While high concentrations of particulate matter were shown to be mostly advected to Paris from Northern and continental Europe (Beekmann et al., 2015), VOCs are expected to be mainly from local origin, due to their shorter lifetime.

50 Over the last decade, several studies have focused on VOCs in the Paris region (Gros et al., 2011; Gaimoz et al., 2011; Borbon et al., 2013; Ait-Helal et al., 2014; Baudic et al., 2016; Languille et al., 2020), but were all carried out over a relatively short timeframe (< 1 year). Measurements in Paris city centre showed that the main VOC sources were motor vehicle exhaust, evaporative sources, wood burning, biogenic sources, solvent use, natural gas and background (Gaimoz et al., 2011; Baudic et al., 2016). An important influence of the air mass origin was pointed out, notably showing that local traffic sources were
55 dominant under oceanic air masses and that under continental air masses, remote industrial pollution was important (Gaimoz et al., 2011); Baudic et al. (2016) and Languille et al. (2020) highlighted the significant contribution of local residential wood burning in the wintertime.

Located about 20 km from Paris city centre, the SIRTa (Site Instrumental de Recherche par Télédétection Atmosphérique) observatory platform is one of the very few suburban sites of ACTRIS. Aerosols (concentration, chemical composition,
60 granulometry, optical properties) and reactive gases (NO_x , O_3) have been monitored at SIRTa for about a decade.



Complementary measurements of VOCs would allow a better understanding of the sources and formation of secondary pollution in this region.

Historically in Europe, VOCs have been monitored using mainly canister samples and gas chromatography for Non-Methane HydroCarbons (NMHC) and carbonyl DNPH tubes for Oxygenated VOCs (OVOCs) in 17 sites of different types: rural, urban, mountain, coastal, remote (Solberg et al., 2021). While these techniques are robust, canister samples and DNPH are providing data only once to twice a week. They allow the analysis of long-term trends in the VOC levels, but it is not possible to capture emission and transformation processes. Online techniques such as Gas Chromatography and Proton-Transfer-Reaction Mass Spectrometry (PTR-MS) enable capturing the temporal variability of NMHC and/or OVOC. PTR-MS instruments were developed in the 1990s by Lindinger et al. (1998) and their short sampling time of a couple of minutes allows to greatly characterize the pollutants' temporal variability. This technique enables the analysis of both OVOCs and NMHC, except for alkanes and light alkenes. Long-term measurements using PTR-MS remain however rather scarce within Europe.

For the start of the long-term PTR-MS measurement at SIRTA, a preselection of more than 30 compounds was done. These include aromatic hydrocarbons, such as benzene and toluene, which are primary compounds emitted by anthropogenic sources, like traffic and wood burning (Kaltsonoudis et al., 2016; Languille et al., 2020). Biogenic VOCs, isoprene and monoterpenes, are also monitored; these correspond to primary compounds as well, but are mainly released by vegetation in summer (Jordan et al., 2009; Steinbrecher et al., 2009). Moreover, oxygenated VOCs such as methanol, acetone, acetaldehyde, acetic acid, – corresponding to primary and secondary compounds that can have biogenic and/or anthropogenic origins (Baudic et al., 2016; Bruns et al., 2017) – are also considered as key variables for ACTRIS.

Here, we present the first long-term PTR-MS measurements in a suburban site in Europe. VOC measurements started in January 2020 at SIRTA, allowing to document and make available, from the ACTRIS data portal, two years of near real-time VOC in situ measurements. The first part of the present manuscript provides details on the instrumental setup, data treatment and quality assurance procedures. Then, a descriptive analysis of the data is proposed. A particular interest is given to the influence of meteorology and air mass origin on the VOCs' loadings, as well as on their seasonal and diurnal variabilities. Finally, a focus is made on the COVID19-induced lockdown period during Spring and Autumn 2020.

85

2 Instrumentation

2.1 Site presentation

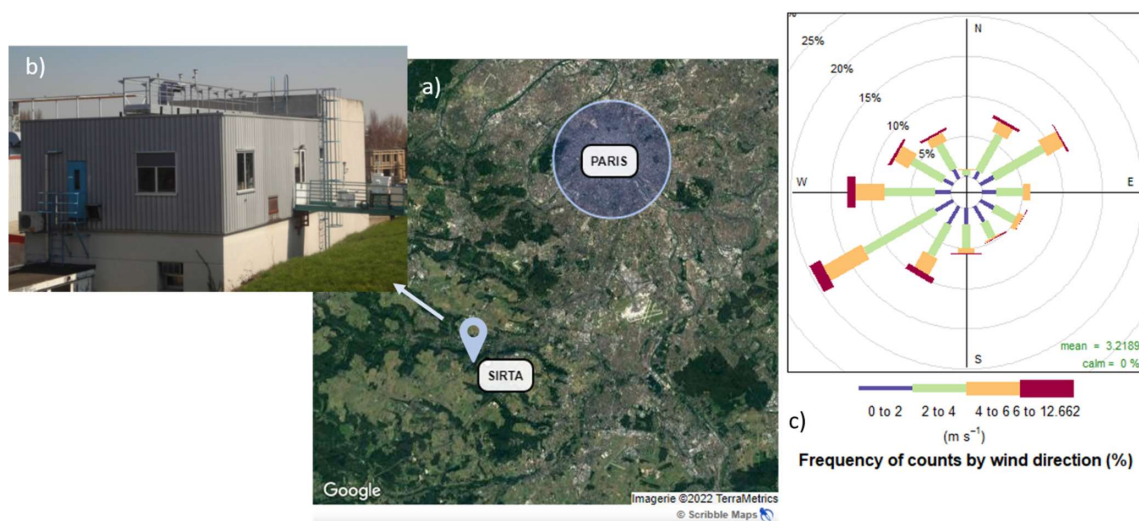
2.1.1 Sampling station

The SIRTA (Site Instrumental de Recherche par Télédétection Atmosphérique) observation platform is located 20 km southwest of Paris (France) and is considered as representative of suburban background conditions in the Paris region (Haefelin et al., 2005; Sciare et al., 2011). It is one of the main ACTRIS national facilities in France. It is composed of a main



site (48.718°N, 2.208°E, 156 m above sea level), for monitoring atmospheric meteorological parameters, as well as for aerosols and clouds remote sensing. Dedicated in-situ observations of aerosols and reactive gases are conducted at the Laboratoire des Sciences du Climat et de l'Environnement (LSCE, 48.709° N, 2.159° E, 162 m above sea level), 4 km away from the main
95 SIRTAsite.

The Paris region is quite densely populated, local residential areas are situated mainly north and east of the station. Highways with important traffic (A6, A10) connect Paris to other cities and pass through the east and south of the station, a national road with important traffic (N118) passes to the east. Forests, agricultural and natural areas are located on the west and south of SIRTAsite, and marine air masses from the Atlantic Ocean can reach the Paris region (Crippa et al., 2013). The station is therefore
100 under different plumes depending on the wind direction, i.e. under regional background and oceanic air masses if the wind comes from the west/southwest, or under Paris and continental plumes if the wind comes from the north/northeast (see Figure 1). In 2020 and 2021, SIRTAsite was respectively 50% and 36% of the time under oceanic (SW) and continental (NE) plumes. Throughout this manuscript, results are shown in universal time (UTC), while local time corresponds to CET (UTC+1) from November to March and to CEST (UTC+2) from April to October.



105

Figure 1: a) Map of the South-West part of the Paris region, location of the SIRTAsite b) Picture of the observatory building c) Wind rose: wind speed and direction occurrences at SIRTAsite for the period 2020-2021



110 2.1.2 Online measurements of aerosol chemical species and inorganic gaseous compounds at SIRTA

Major submicron aerosol chemical species, i.e organic matter (OM), nitrate, sulfate, ammonium, and chloride, have been measured using a quadrupole Aerosol Chemical Speciation Monitor (Q-ACSM) since 2011. The operating principle of the instrument is described in Ng et al. (2011), while its setup at SIRTA and first years' results can be found in Petit et al. (2015) and Zhang et al. (2019).

115 For this study, complementary information on equivalent black carbon (eBC) concentrations and sources is provided by co-located multiwavelength Aethalometer (Magee Scientific). Since 2013, an AE33 model has been used, as described in Petit et al. (2015) and Zhang et al. (2019). Therefore, eBC could be discriminated between its two main combustion sources, i.e. fossil-fuel (BC_{ff}) and wood burning emissions (BC_{wb}), using the Aethalometer model (Sandradewi et al., 2008; Favez et al., 2010; Sciare et al., 2011; Drinovec et al., 2015). For these calculations, the absorption Angström exponent values used, in the
120 wavelength range of 470-950nm, were 0.9 and 1.85 for BC_{ff} and BC_{wb} respectively, based on Petit et al. (2021).

Nitrogen monoxide and dioxide (resp. NO and NO₂) have been monitored since 2012 using chemiluminescence NO₂/NO/NO_x analyzer (model T200UP, Teledyne API, USA).

2.2 General description of a PTR-MS

125 With the aim of characterizing VOC levels on a real-time and long-term basis, a Proton-Transfer-Reaction Quadrupole Mass Spectrometer (PTR-Q-MS, Ionicon Analytik, 2010) has been implemented at SIRTA. The technique was first used by Lindinger et al. (1998), where it is comprehensively described. Briefly, ambient air is pumped in the drift chamber, where gaseous molecules M which have a proton affinity greater than that of water react with protonated water molecules (H₃O⁺) produced in the ion source, to form ionized MH⁺. Protonated compounds MH⁺ are then driven through a quadrupole, where
130 they are separated according to their mass-to-charge ratio (m/z). Finally, they pass through the electron multiplier (SEM) for detection. The obtained raw signal is in counts per second (cps) per m/z. This soft ionization process induces low fragmentation in the drift tube.

Regular blanks need to be performed in order to account for instrumental background, which can be significant for some m/z. These blanks are usually done by passing clean air through the inlet line and conducted ideally every few hours and at least
135 once a day. In order to calibrate the instrumental response to ambient VOC mixing ratios, a bottle containing a standard gas mixture can be diluted in clean air to perform several concentration steps. Usually, the standard mixture doesn't contain all measured compounds; therefore, another method is applied, the so-called "kinetic approach", which uses a transmission curve. This approach, detailed in Taipale et al. (2008) and summarized in Text S1, consists of using the calibrated compounds' transmission to retrieve the other compounds' transmission and determine their sensitivity.



140 2.3 Operating conditions of the PTR-Q-MS at SIRT A

2.3.1 Sampling conditions

The sampling line is made of PFA (perfluoroalkoxy), has a total length of 6 metres and samples at about 15 m high above ground level. A pump provides a flow of about $8 \text{ L} \cdot \text{min}^{-1}$, thus ensuring a residence time for the air in the tube of about 3 seconds. The line is heated at 50°C to avoid condensation. A VALCO valve (Interchim, France) allows to automatically switch
145 from ambient air, blank and standard measurements.

2.3.2 Instrument parameters

For long-term measurements at SIRT A, the drift pressure (p_{drift}) is set to 2.2 mbar, drift voltage (U_{drift}) is set to 600V and drift temperature (T_{drift}) is set to 60°C , resulting in an E/N ratio (parameter corresponding to the ratio of the electric field to the number density of the gas in the drift tube) of 134 Td. A lower E/N would induce more humidity in the instrument, while a
150 higher E/N would result in more fragmentation of the compounds (Taipale et al., 2008). Other parameters such as water flow, ion source current, voltages at the entrance and exit of the drift chamber and detector voltage are regularly adjusted, in order to maintain the instrument functioning in an optimized way (See Table S1).

2.3.3 Measured mass-to-charge ratios

The PTR-Q-MS can work either in scan mode, in which case all m/z are scanned in a defined range; or the m/z that will be
155 measured are defined ahead. The scan mode is often used to investigate which m/z have a distinct signal in sampled air; however, a complete scan cycle, with a dwell time of five seconds per m/z , would take 11 minutes. Throughout the measurement period, it was observed that a dwell time of five seconds per mass can result in a low sensibility, and so a dwell time of ten seconds per mass was preferred, which would result in a resolution time of 22 minutes. In order not to lose the advantage of a resolution time $< 15 \text{ min}$, the m/z selection method was chosen.

160 The selection for measured m/z was therefore performed based on previous studies and using the scan mode for a couple of days before starting the long-term measurements. Mass-to-charge ratios corresponding to the main VOCs present in ambient air (de Gouw and Warneke, 2007; Blake et al., 2009; Yuan et al., 2017b), m/z highlighted as markers for specific sources: traffic, wood burning, agricultural activities (Bruns et al., 2017; Kammer et al., 2019; Languille et al., 2020), and m/z that had significant level and variability during the scan, were selected for the PTR-MS measurements. This resulted in 37 mass-to-charge ratios measured, the first 6 being for instrumental diagnostic purposes: m/z 21, 25, 30, 32, 37, 55, 31, 33, 42, 45, 46,
165 47, 57, 58, 59, 60, 61, 63, 69, 71, 73, 75, 79, 81, 83, 85, 87, 93, 97, 99, 107, 111, 121, 137, 139, 147, 151. The resulting time resolution was 2.6 min from January to November 2020 and 5.2 min from December 2020 on, when the dwell time was increased from 5 to 10 seconds per m/z .



2.3.4 Blanks and calibration

- 170 A Gas Calibration Unit (GCU, Ionimed Analytik, Austria) was used for 1-hour blanks every 13 hours and for regular calibrations, about once a month: a VOC standard mixture was injected through the dilution system to perform steps at different volume mixing ratios (VMR, ranging from 1 to 20 ppb). Different standards were used throughout the study period (see Table S2); the obtained sensitivity coefficients did not vary for more than 21% from one standard to another (mean value: 7%). An NPL-certified standard (National Physical Laboratory, 2021) was used for comparison; the difference of sensitivity with the
- 175 other standard ranged from 0 to 18%, depending on the compounds (mean value: 7%). This standard was also used to infer the repeatability of the measurement over 3 days, with conditions (i.e. lab temperature) that might vary a little; the obtained coefficients of variation ranged from 1 to 26% (mean value: 7%). In addition, the influence of humidity on the sensitivity was investigated by performing calibrations at set relative humidity (RH) of 30%, 60% and 90%. The obtained sensitivities did not vary more than 10% between each test (mean value: 3%).
- 180 Once the ambient counts per second (cps) are normalized by primary ions and humidity, the obtained blanks and sensitivities are linearly interpolated and are used to retrieve the ambient VMR.

2.4 Quality control

2.4.1 Internal quality control and maintenances

- The measurements, as well as the instrument parameters (pressures, voltages, source intensity, water flow) are checked at least
- 185 twice a week, in order to diagnose an issue with the PTR-Q-MS. A target bottle, containing stable ambient air, is sampled once per week as a secondary standard, in order to check the stability of the measurements. These measurements show a mean coefficient of variability of 33% over the whole 2020-2021 period.

- Throughout the two-year period, the PTR-Q-MS encountered a couple of shutdowns due to common mild dysfunctions, with a usual downtime of around a week. Nevertheless, two major breakdowns occurred. One from April to June 2020, when
- 190 troubleshooting and maintenance were not possible due to the Covid-19 lockdown; the second one from June to August 2021, because the diagnosis of the issue was difficult. Considering periods where the PTR-Q-MS was down, and the data that had to be invalidated, this resulted in a data coverage of 61% between the start of the measurements and the end of 2021. The data coverage per season, considering two whole years expected, is 74% in winter, 37.5% in spring, 42% in summer, and 85% in autumn.

195 2.4.2 PTR-ToF-MS campaigns

Isobaric compounds cannot be separated with a quadrupole mass spectrometer, but they can be with time-of-flight mass spectrometry (ToF-MS). For example, at m/z 69 two important compounds are detected: isoprene (C_5H_8) and furan (C_4H_4O).



While isoprene is the main biogenic compound, furan can be emitted by biomass burning in winter (Bruns et al., 2017; Languille et al., 2020; Coggon et al., 2019).

200 In order to separate and investigate isobaric compounds throughout the year, a PTR-ToF-MS (Ionicon, 1000) was deployed during several months in 2020. This paper does not intend to intercompare both PTR-MS at SIRTÀ, the PTR-ToF-MS was only used here to determine the contribution of isobaric compounds to their nominal mass, and tentatively attribute compounds to measured mass-to-charge ratios. A first campaign took place from 17/02/2020 to 16/03/2020, a second one from 10/04/2020 to 20/07/2020 and a third one from 06/11/2020 to 16/12/2020. A 16-m PFA sampling line, heated at 50°C was used to sample
205 at the same height as the PTR-Q-MS. A pump provided a flow of 22 L·min⁻¹, thus resulting in a residence time of about 3 seconds. Blanks were performed manually, using a catalytic converter (Zero air generator, Parker, France) once every other working day during the campaigns, except during the lockdowns (16/03/2020 to 11/05/2020, and 30/10/2020 to 15/12/2020) when they were performed once to twice a week. Calibrations were done about once a month using the internal dilution system.

2.4.3 Tentative attribution of mass-to-charge ratios

210 VOCs were tentatively attributed to the measured *m/z*, based on the literature and on the PTR-ToF-MS measurements. All *m/z*, the attributed compound(s), and their calculated detection limit and uncertainties are given in Table 1. A thorough discussion for each *m/z* is provided in Text S3. Specific nominal masses with different contributions per season are highlighted in Table 2 and *m/z* 69 is discussed below.

m/z 69 corresponds to C₄H₄O: furan and C₃H₈: isoprene and fragments of methylbutenol (MBO), but PTR-ToF-MS
215 measurements showed that MBO is negligible (see discussion of *m/z* 87 in Text S3). Furan is emitted by biomass-burning activities and has highest contributions in autumn and winter; while in spring and summer, *m/z* 69 can be almost exclusively attributed to isoprene, due to its important biogenic source, although it can also be emitted by anthropogenic sources (Borbon et al., 2001; Wagner and Kuttler, 2014; Panopoulou, 2020).

2.4.4 Detection limit and uncertainties calculation, ACTRIS quality control

220 The detection limits and uncertainties for each *m/z* were calculated according to ACTRIS guidelines for PTR-MS (in preparation). Table 1 presents the results for all compounds: the detection limit ranged from 6 to 221 ppt and the uncertainties ranged from 14 to 73%.

An internal quality check is performed on all *m/z*, consisting in carefully verifying the obtained data. An external quality control is also performed by ACTRIS on 12 masses corresponding to the following compounds: benzene, propenal+C₄H₈,
225 isoprene+furan, C₈-aromatics, monoterpenes, toluene, acetonitrile, acetaldehyde, acetone, MEK, methanol and MVK+MACR. Thus, the dataset is compliant with their expectations and can be available on Ebas database.



230 **Table 1: List of mass-to-charge ratios measured, their corresponding name in this paper, their mean detection limit (LOD) and mean error. Compounds in bold are quality checked by ACTRIS**

mz	name(s)	mean LOD (ppt)	mean LOD ($\mu\text{g}/\text{m}^3$)	mean error (%)
mz_31	Formaldehyde proxy	58	0.074	37
mz_33	Methanol	221	0.300	16
mz_42	Acetonitrile	9	0.016	16
mz_45	Acetaldehyde	47	0.088	18
mz_46	m46	54	0.104	33
mz_47	Ethanol + Formic acid	67	0.131	33
mz_57	C4H8 + Propenal	23	0.055	20
mz_58	Allylamine	6	0.014	69
mz_59	Acetone	17	0.042	14
mz_60	Trimethylamine	11	0.028	34
mz_61	Acetic acid	34	0.087	31
mz_63	DMS	20	0.054	41
mz_69	Isoprene + Furan	37	0.107	21
mz_71	MVK + MACR	10	0.029	25
mz_73	MEK	14	0.044	19
mz_75	C3H6O2	16	0.049	33
mz_79	Benzene	21	0.068	19
mz_81	MT's fragments	8	0.026	33
mz_83	Methylfuran + C6H10	10	0.036	67
mz_85	Methylbutenone	9	0.033	36
mz_87	Butanedione + Methacrylic acid	40	0.148	36
mz_93	Toluene	24	0.095	20
mz_97	Furfural	11	0.047	35
mz_99	Furandione + Furfuryl alcohol	14	0.057	36
mz_107	C8-aromatics	36	0.161	23
mz_111	Benzenediol	30	0.138	42
mz_121	C9-aromatics	31	0.156	31
mz_137	Monoterpenes	37	0.216	34
mz_139	Nopinone	24	0.142	73
mz_147	Dichlorobenzene	26	0.160	43
mz_151	Pinonaldehyde	46	0.292	48



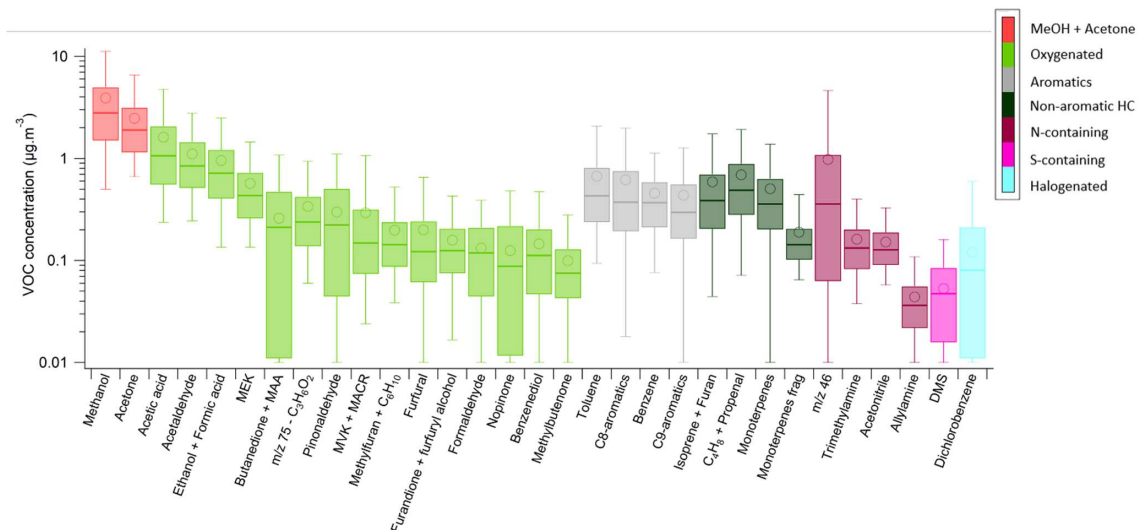
235 **Table 2: Specific m/z with different compound contributions per season**

m/z	Compound names	Formula	Winter (%)	Spring (%)	Summer (%)	Autumn (%)	Year (%)
46	PAN fragments	NO ₂ ⁺	84	81	NA	80	81
	Formamide	CH ₃ NO	15	17	NA	18	17
	Dimethylamine	C ₂ H ₇ N	1	2	NA	2	2
47	Formic acid	CH ₂ O ₂	42	92	94	61	82
	Ethanol	C ₂ H ₅ OH	58	8	6	39	18
57	Propenal	C ₃ H ₄ O	25	16	37	30	26
	Butene/HC fragments	C ₄ H ₈	75	84	63	70	74
69	Furan	C ₄ H ₄ O	67	6	4	47	23
	Isoprene	C ₅ H ₈	33	94	96	53	77
83	Methylfuran	C ₅ H ₆ O	100	50	55	80	73
	Cyclohexene/HC fragments	C ₆ H ₁₀	0	50	45	20	27
107	Benzaldehyde	C ₇ H ₆ O	0	45	34	3	19
	C8-Aromatics	C ₈ H ₁₀	100	55	66	97	81

3 Volatile Organic Compounds phenomenology at SIRTa

3.1 Descriptive analysis

Levels and statistical variability of the measured Volatile Organic Compounds (VOC) are shown in Figure 2 for the two-year period. The compounds were grouped, depending on their nature, into 7 families: methanol + acetone, oxygenated, aromatics, non-aromatic hydrocarbons, nitrogen-containing, sulfur-containing and halogenated. Methanol and acetone were separated from the other oxygenated VOC due to their concentration (2-3 times higher) and for the sake of clarity in the next graphs. Note that S-containing and halogenated groups contain only dimethylsulfide and dichlorobenzene, respectively. Due to their low levels and noisy signals, they are not presented in the figures for the rest of the paper. The statistics (mean, median, 5th, 25th, 75th and 95th percentiles) for all m/z are given Table S3. Unlike in the instrumentation section, where the values of the VOCs are expressed as the VMR in ppb, in the results they are converted to concentrations in $\mu\text{g}\cdot\text{m}^{-3}$. This conversion is presented in Text S2.



250 **Figure 2: Statistical distribution of VOC measurements during the two years period. Boxes represent 25th and 75th percentiles, the line is the median. Whiskers represent 5th and 95th percentiles and the circles represent the mean value.**

Methanol and acetone showed the highest levels with mean values above $2 \mu\text{g}\cdot\text{m}^{-3}$, as previously observed in the Paris region (Gros et al., 2011; Baudic et al., 2016; Languille et al., 2020). The group of oxygenated compounds presents a large variability of concentrations: acetic acid, acetaldehyde, and ethanol + formic acid have a mean concentration of around $1 \mu\text{g}\cdot\text{m}^{-3}$, while nopinone, benzenediol, and methylbutenone have a mean concentration of around $0.1 \mu\text{g}\cdot\text{m}^{-3}$. The levels of the different aromatic compounds and groups are very similar. Within the non-aromatic hydrocarbons, monoterpenes have roughly the same boxplot values than isoprene, although isoprene is expected to be the most important biogenic compound in the atmosphere. This could be explained by the high variability of m/z 137, due to its important concentration in the wintertime.

260

Figure 3 displays the contribution of the different VOC families to the total VOC concentration, per class of total VOC concentration. The contributions of methanol + acetone and oxygenated compounds don't vary a lot from one class to the other. Nitrogen-containing compounds increase with increased total concentration until $30 \mu\text{g}\cdot\text{m}^{-3}$, and then stabilize. On the other hand, aromatic compounds decrease with increased total concentration; their highest contribution is observed for the smallest total concentration. These results were compared with the particles' composition, in terms of organic matter, NO_3 , NH_4 , SO_4 , Cl and black carbon, per class of total concentration. The tendencies observed for the VOCs are similar to the particulate composition, with black carbon contributing more to lowest particle concentrations, and nitrate increasing with

265



increasing total aerosol concentration until $50 \mu\text{g}\cdot\text{m}^{-3}$ (Petit et al., 2015). Black carbon and aromatic VOCs are expected to have the same sources and to correlate with each other (Languille et al., 2020), and this result could indicate common sources or (trans)formation processes for nitrate and nitrogen-containing VOCs.

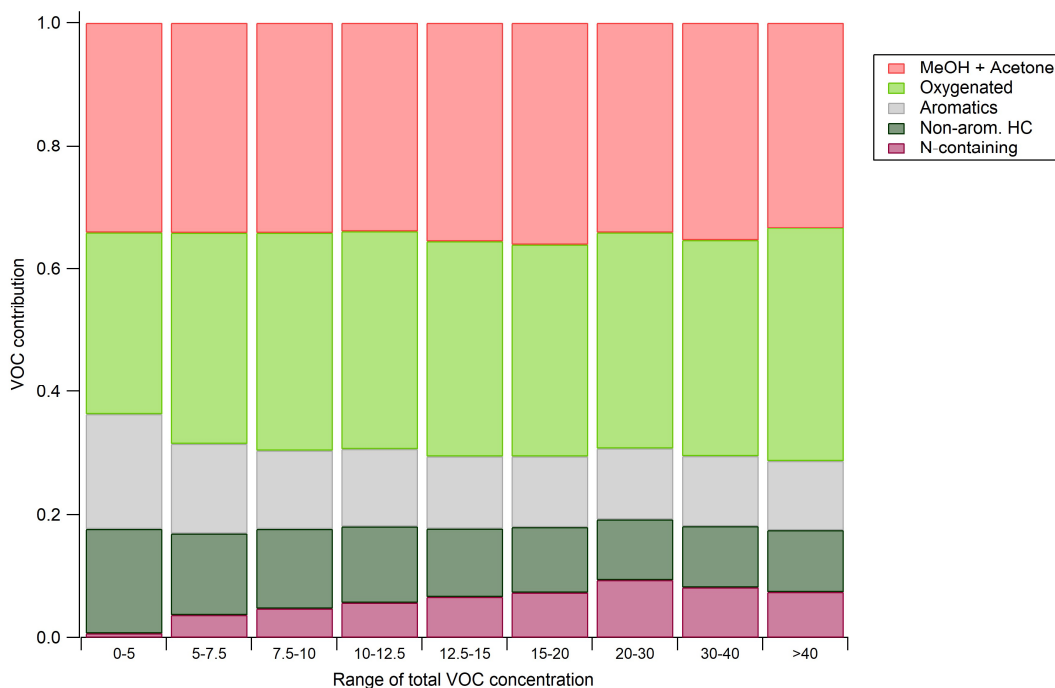


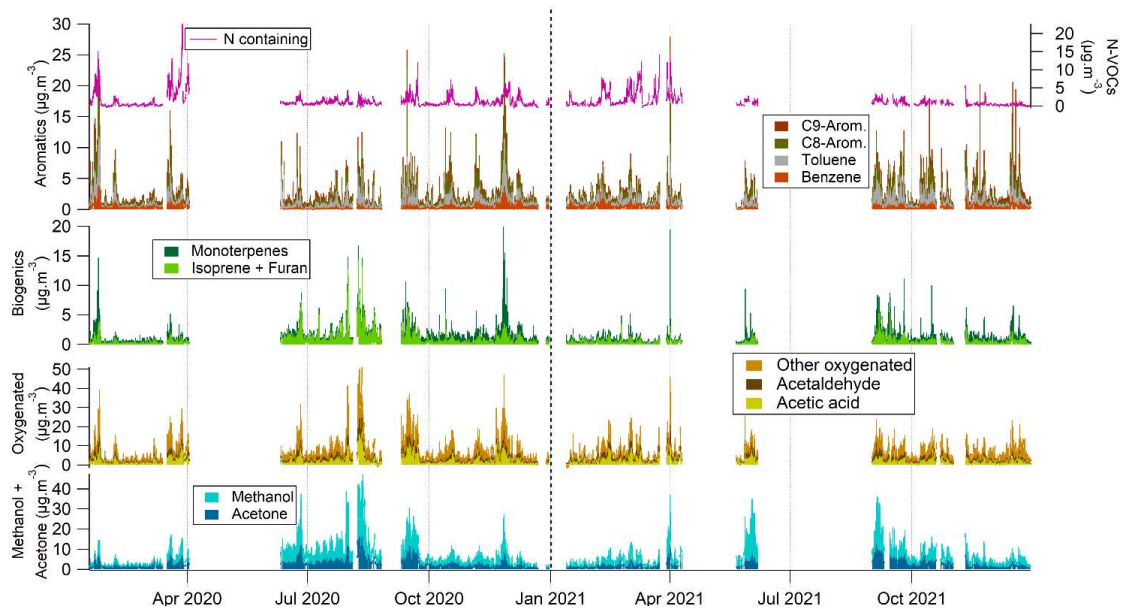
Figure 3: Contribution of VOC families to the total concentration per class of total VOC concentration

3.2 Overview of VOC variability and influence of air mass origin

The time series over 2020 and 2021 of the concentrations of VOCs per family are shown on Figure 4. Methanol and acetone show a high variability, with cumulated levels up to $40 \mu\text{g}\cdot\text{m}^{-3}$ in the summertime, while they are on average lower than $10 \mu\text{g}\cdot\text{m}^{-3}$ in winter. Conversely, the other oxygenated compounds have similar levels throughout the year, as they come from both biogenic and wood burning sources. Aromatic compounds dramatically increase during pollution episodes, empirically defined here as a period of at least 3 successive days with a daily maximum value of aromatics $> 5 \mu\text{g}\cdot\text{m}^{-3}$ and at least one daily mean value $> 5 \mu\text{g}\cdot\text{m}^{-3}$. These events especially occur in autumn/winter (11 events in autumn/winter vs 4 in spring/summer), due to lower temperatures, more active sources and a lower boundary layer (Baudic et al., 2016; Languille et al., 2020), inducing less dispersion of the pollutants. Nitrogen-containing compounds increase in Spring, most probably due to agricultural sources being important in this season, as is also seen for ammonium nitrate (Petit et al., 2015; Beekmann et al.,



2015); but they also increase during some of the pollution events (i.e. at the end of January 2020), which could indicate other anthropogenic sources.



285

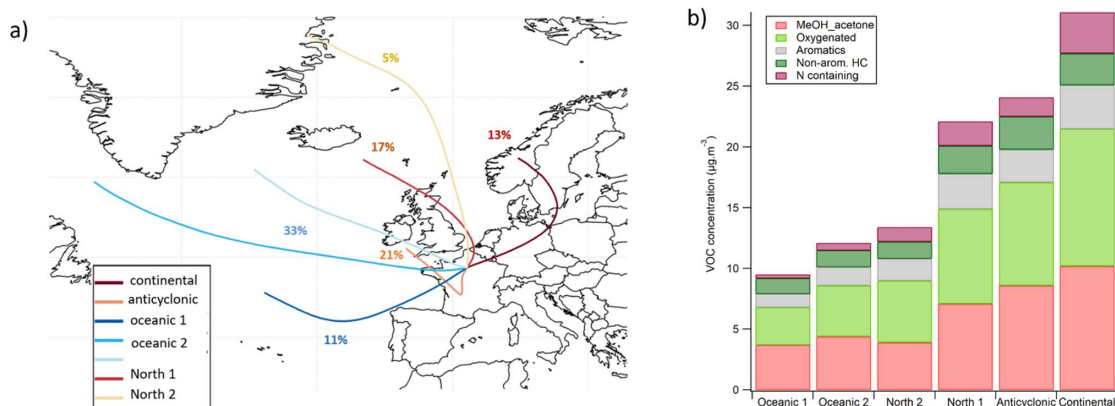
Figure 4: Time series of cumulated concentrations of VOCs within the different families. The black dotted line marks the separation between 2020 and 2021 and the grey dotted lines mark every 3 months

The influence of air mass origin was investigated to better understand the levels and variability of the VOCs. This was done using a cluster analysis from ZeFir (Petit et al., 2017), based on the HYSPLIT back trajectories reaching SIRTAs calculated every 3h from January 2020 to December 2021.

290

In total, seven clusters were obtained (see Figure 5 a) below), corresponding to: continental air masses, an anticyclonic cluster, three oceanic air masses of which two were grouped into oceanic 1 and oceanic 2, and two air masses from the North (North 1 & 2). Continental and North 1 are expected to be polluted air masses, due to their probability of passing over Paris and other dense urban areas in the Benelux, thus accumulating pollution along the way. The local anticyclonic cluster is also expected to be polluted, due to local sources and more stable meteorological conditions. On the other hand, both oceanic clusters and North 2 are expected to be clean, due to less anthropogenic sources. The oceanic air masses were dominant (44% in total), followed by northern air masses (22% in total), anticyclonic (21%) and the continental cluster (13%). Continental, North 1 and North 2 are of higher frequency in Spring (around 40% of the year) and Oceanic 1 is more frequent for the winter season (40%).

295



300

Figure 5: a) Map of obtained air mass clusters for the period 2020-2021 (ZeFir) b) VOC concentration and composition per cluster

The contribution to each cluster of the concentration of the VOC families is shown in Figure 5 b). The mean concentration of each m/z for each cluster is given Table S4. As expected, the most polluted clusters were continental, anticyclonic, and North 1 (Figure 5b). While oceanic air masses are the most frequent, they contribute the least to the VOC levels. There doesn't seem to be a real difference in the composition of the different clusters, however small changes can be seen. For instance, nitrogen-containing compounds are dominated by continental air masses (see Figure 6), which could indicate agricultural sources located in that direction. Another possibility is the formation of alkylnitrates (including PAN) by atmospheric aging of hydrocarbons in the presence of NO, measured as NO_2^+ fragment at m/z 46 (Kastler and Ballschmïter, 1998; Müller et al., 2012). Aromatic VOCs contribute more to the northern air masses. Non-aromatic hydrocarbons contribute more to the anticyclonic and oceanic 1 air masses, indicating local or regional sources, and/or short lifetime.

305
310

3.3 Seasonal and diurnal variability of the VOC

In this section, the seasonal variability of individual VOC is explored, these VOCs being from different families, having different sources, and presenting different variabilities. Figure 7 presents the level and statistical variability per months of 2020 and 2021 of methanol, benzene, isoprene + furan, MVK+MACR, toluene and monoterpenes, as well as temperature, relative humidity and the mixed layer height (MLH).

315

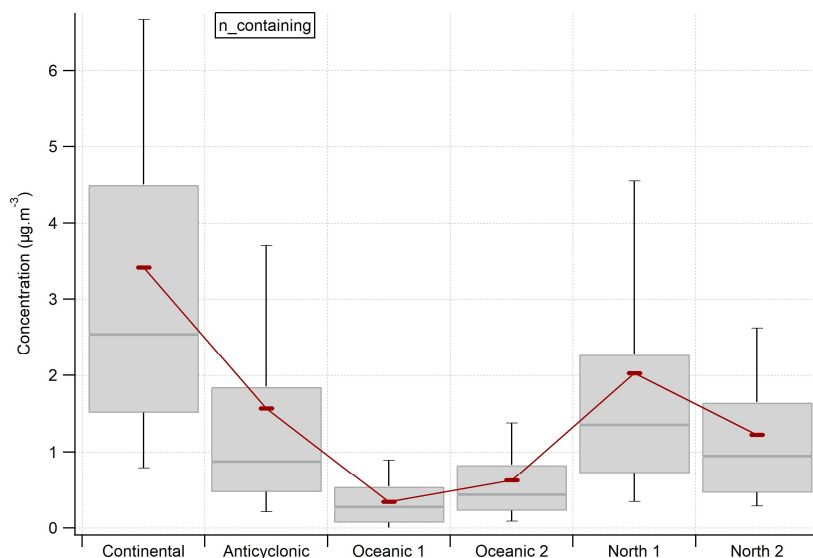


Figure 6: Statistical distribution of N-containing compounds per air mass cluster

320 In this region of the world, the ambient temperature increases from spring (MAM) to summer (JJA), then decreases in autumn
(SON) until winter (DJF). The temperature in April and May 2020 was higher than in 2021 and similar to temperatures
observed in June; spring 2020 was abnormally warm: the mean temperatures recorded in Paris showed an increase of 4.2°C in
April 2020 and 1.6°C in May, compared to the 1981–2010 normal (infoclimat.fr, 11/04/2022). For the other months, the
temperature was relatively similar between 2020 and 2021. The mixed layer height (MLH) increases from April to September
325 and decreases during autumn and winter.

Methanol has a similar seasonal variability than the temperature, with higher levels in summertime due to temperature-driven
biogenic emissions and production of methanol by photooxidation of other species, a process more important in summer due
to increased sunlight. Moreover, high levels of methanol in May 2021 despite the temperature being lower than in the summer
months indicates that temperature is not the only parameter driving the emission and formation of methanol.

330

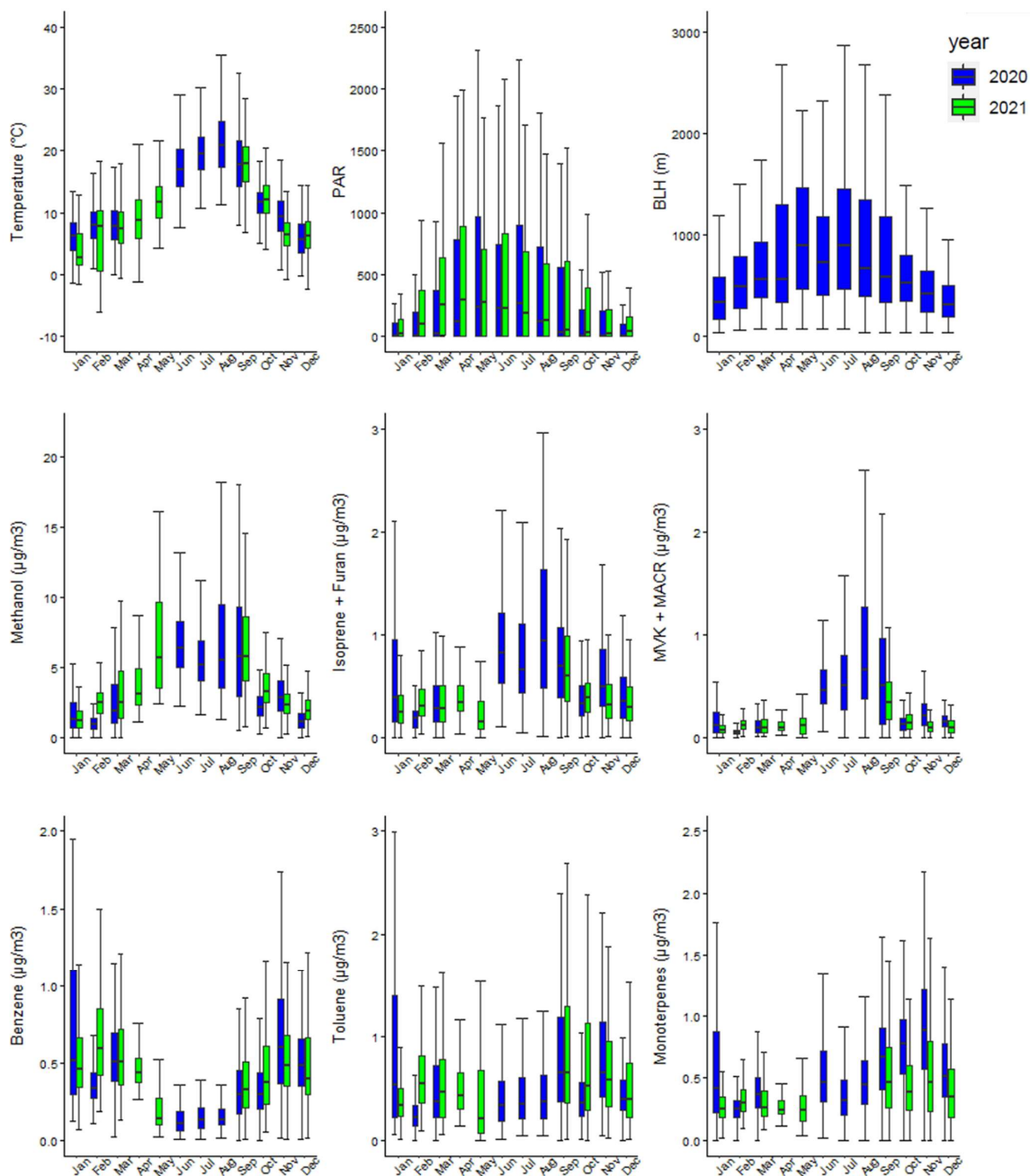




Figure 7: Monthly distribution of VOC, temperature, photosynthetically active radiation (PAR, in $\mu\text{mol}\cdot\text{s}^{-1}\cdot\text{m}^{-2}$), and boundary layer height for 2020 (blue) and 2021 (green). Boxes represent 25th and 75th percentiles, the line is the median. Whiskers represent 5th and 95th percentiles

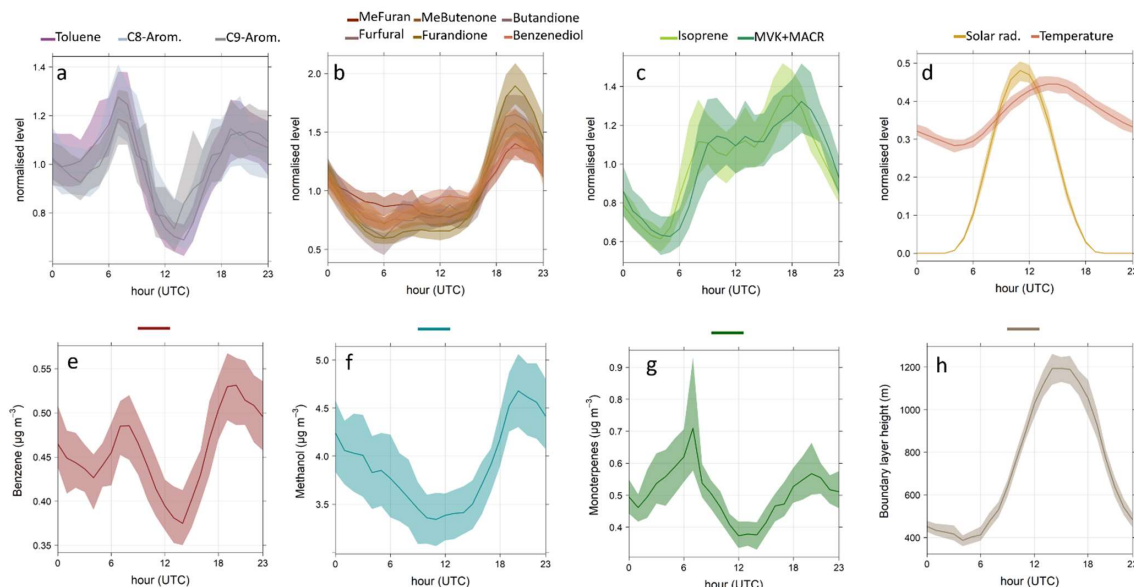
335

The sum of isoprene and furan also shows a great variability, with increased levels during summer (June to September), due to isoprene being widely emitted by biogenic sources when the temperature and solar radiation are highest. In the wintertime, non-negligible levels of m/z 69 are explained by furan emitted from wood burning. MVK+MACR have very low levels during
340 winter, but increase a lot in the summer months, due to their production through the rapid photo-oxidation of biogenic isoprene. Benzene increases from September to April; due to more active sources in winter like residential wood burning (Languille et al., 2020) and less dispersion when the boundary layer is low, which is supported by wood burning tracers such as furfural and benzenediol showing the same tendency (see Figure S1). Toluene does not display a seasonal pattern as strong as benzene, although it also has higher levels in autumn and winter. Its main source, traffic, is important all year long and the more stagnant
345 conditions in autumn and winter induce pollutant accumulation.

Finally, monoterpenes, which are considered to be important biogenic compounds, are expected to have higher levels in summer (Jordan et al., 2009; Steinbrecher et al., 2009; Chen et al., 2020). Here, high levels of monoterpenes in summer are indeed observed, but they increase in autumn and winter. This suggests that monoterpenes could have anthropogenic sources
350 in our study, especially in autumn and winter. Their relatively low levels in summer could also indicate their important reactivity with OH and O₃, leading to possible formation of secondary organic aerosols (Yu et al., 1999; Larsen et al., 2000; Orlando et al., 2000; Mahilang et al., 2021). Moreover, a difference between 2020 and 2021 is observed for the months of September to December, which is barely seen for other VOCs. The seasonal cycle of monoterpenes resembles that of toluene and C8-aromatics (see Figure S1), with high levels from September to June but also shows discrepancies resulting in unclear
355 behaviour of monoterpenes. This is an interesting result to take into account for modelling.

The investigation of the diurnal profiles of some specific compounds might also give indications on their sources and on processes governing their levels in the atmosphere.

Figure 8 a) represents the diurnal profile of aromatic compounds (toluene, C8- and C9-aromatics), markers for the traffic source, which peaks during the morning (5–8 AM UTC) and evening (3–8 PM UTC) rush hours. Their level stays high during
360 the night due to the lower boundary layer. During the day, aromatic compounds decrease due to their dilution enhanced by the boundary layer dynamics and due to their fast reaction with OH and O₃. The gaseous traffic markers correlate with each other, in the wintertime, with a R² of 0.6–0.8, and they correlate with the fossil fuel fraction of black carbon (BC_{ff}) with a R² > 0.7 (see Table S5).



365

Figure 8: Diurnal profiles for the whole studied period at SIRT: a) VOC associated with a traffic pattern (toluene, C8-aromatics, C9-aromatics), b) VOC associated with a wood burning pattern (methylfuran, methylbutenone, butanedione, furfural, furandione, benzenediol), c) Isoprene and its oxidation products (methyl vinyl ketone + methacroleine), d) Solar radiation and temperature, e) Benzene, f) Methanol, g) Monoterpenes, h) Boundary layer height (data only available in 2020). The line represents the mean and the shaded area corresponds to 95% confidence interval. Diurnal cycles a, b, c and d were normalised by the mean.

370

Figure 8 b) presents several compounds – methylfuran, methylbutenone, butanedione, furfural, furandione, benzenediol – markers for the wood burning source (Languille et al., 2020). Their diurnal cycle shows a peak in the evening (3–8 PM UTC), due to people coming home from work and using residential wood burning for heating. Unlike the traffic markers, the wood burning-related VOCs decrease during the night, which could be explained by their reaction with NO_3 , an important nighttime oxidant, that leads to partitioning into the particle phase (Joo et al., 2019; Mayorga et al., 2021). Other compounds such as methanol, acetaldehyde, acetic acid, and furan were also highlighted as wood burning markers by Languille et al. (2020), but although this may be their main source in winter, their overall diurnal cycle displays a different pattern due to additional sources like vegetation or solvent use, throughout the year. The compounds highlighted here as wood burning markers correlate each with the wood burning fraction of black carbon (BC_{wb}) during winter with a R^2 of about 0.7, except for butanedione (see Table S5).

375

On Figure 8 c), the sum of isoprene and furan shows a more biogenic diurnal cycle because isoprene is dominant (77%), with an increasing level in the morning due to enhanced emission with higher temperature and solar radiation. Once the plateau is reached around 8 AM UTC, the balance between fresh emissions of isoprene and its removal by OH results in levels staying the same. A peak in the late afternoon (3–6 PM UTC) is observed, which could be explained by a shift in this balance due to



385 lower OH concentration (Jordan et al., 2009). After 6 PM UTC, isoprene emissions drop rapidly due to lower temperature and solar radiation, so its level decreases. The diurnal profile of the sum of MVK and MACR (isoprene oxidation products) is very similar to the one of isoprene, although a shift of 1-1.5h between both m/z is observed (Verreyken et al., 2021), corresponding to the lifetime of isoprene in the presence of OH (Seinfeld and Pandis, 2006).

Figures 8 e), f) and g) show the diurnal cycle of different compounds that have mixed sources. Benzene is emitted by both traffic and wood burning (Languille et al., 2020), its diurnal profile shows the typical double peak of traffic-like profiles, but its evening peak is higher, suggesting the influence of the wood burning source. Methanol is always present in important amounts and therefore its diurnal cycle is not marked by a particular source. However, a higher level during the night with respect to the day could indicate an impact of the boundary layer, less oxidation during the night than during daytime, and/or the influence of the wood burning source.

395 Monoterpenes are commonly considered to be mainly emitted by vegetation (Guenther et al., 1995), especially in summer. Figure 8 g) shows that their diurnal cycle is not similar to that of other biogenic compounds at SIRTA. This could be explained by their different emission processes (Steinbrecher et al., 2009; Chen et al., 2020), or by a significant influence of anthropogenic sources, as already suggested in Figure 7. In this study, monoterpenes have a traffic-like diurnal pattern, with morning and evening rush-hour peaks, which could be explained by a traffic source, but more probably by mixed biogenic and anthropogenic sources. Previous studies in urban areas highlighted anthropogenic sources for monoterpenes such as wood burning, domestic solvent use and traffic (Hellén et al., 2012; McDonald et al., 2018; Panopoulou, 2020; Borbon et al, submitted). Panopoulou et al, 2020 notably estimated for Athens an anthropogenic fraction of alpha-pinene of 97% and 70% during winter and summer, respectively. In this study, we show that for the Paris region, the anthropogenic sources of terpenes are also significant. The decrease of monoterpenes during the day and at night can be partly due to their reaction with atmospheric oxidants (OH, O₃, and NO₃) that may lead to important formation of secondary organic aerosols (Mahilang et al., 2021).

These two years of VOC measurements gave information on the seasonal and diurnal variabilities of the different measured compounds, as well as the influence of meteorology and air mass origin on their levels. The measurement period comprises two Covid19-induced lockdowns in Spring and Autumn–Winter 2020, during which the decrease of human activity and change in human behaviour might impact the levels and variability of VOCs. In the next section, these periods will be investigated.

3.4 Covid-19 lockdowns

To reduce the spread of the coronavirus, a strong lockdown was established in France from March 17th to May 10th 2020 included, during which all “non-essential” activities and industries were shut down with a stay-at-home obligation. A second lockdown was established in France from October 30th to December 15th, where going to work was possible but restricted and a curfew was set up in the evening and on the weekends.



The Spring lockdown period corresponded to the occurrence of unusually high temperatures and sunny days, compared to normal conditions over Europe (Barré et al., 2020). Therefore, to quantify a change in pollutants' levels due to the lockdown, the meteorology should be considered (Gkatzelis et al., 2021). At the SIRTA site, such a study was done on PM₁, BC, NO_x, and O₃, thanks to the long dataset available (Petit et al., 2021). This cannot be done for VOCs due to the shortness of the reference and lockdown periods covered by our PTR-MS measurements. Instead, meteorological conditions and air mass origin during this event were studied, as well as the diurnal cycle of some key VOCs before and during the lockdown.

Figure 9 shows the temperature, wind speed and direction, VOC concentrations, and PM₁ composition and concentrations during the month of March 2020. The wind origin and speed occurrences were plotted as wind roses for the first and last two weeks of March (respectively before and during the lockdown).

The concentrations of all groups of VOCs, as well as particulate components, increased suddenly at the start of the lockdown, compared to the period before. There was a drastic change in the wind direction: in the first two weeks of March, wind was coming from the south-west, bringing clean oceanic air masses; while during the last two weeks of March, wind was coming from the north-east, bringing polluted continental and Parisian air masses. This, together with meteorological conditions favouring the accumulation of pollutants (relatively steady winds with a wind speed on average of 3.8 m·s⁻¹, dry conditions with a mean relative humidity of 55%), may explain the increased pollutant levels. Oxygenated and nitrogen-containing VOCs, as well as methanol + acetone increase significantly at the start of the lockdown, especially N-containing compounds on March 28th. On this day, an important increase in particulate nitrate (NO₃⁻) is observed, which was allocated to advected continental pollution (Petit et al., 2021).

Given the difference in the meteorological conditions before and during the lockdown, a quantitative study of the impact of the lockdown on the VOCs cannot be done; however, the diurnal cycle of markers for specific sources in winter were investigated before and during the lockdown. In addition, the diurnal cycles for the second lockdown were also studied.

Figure 10 shows the diurnal profiles of markers for the traffic and wood burning sources for a non-lockdown period with typical background conditions (1–13 March 2020), for periods during the first (17–31 March 2020), and second (30 October–15 December 2020) lockdowns. These profiles are normalised by the mean value, because the periods are not under the same air masses and are not intended to be compared on a quantitative basis. The diurnal cycles of toluene, NO₂, and the fossil fuel fraction of black carbon (BC_{ff}) before the lockdown show typical traffic profiles with morning and evening rush hour peaks. During the Spring lockdown, the diurnal cycles of these compounds seem to have changed, especially for BC_{ff}, which doesn't present a double peak profile anymore. This could be due to an important decrease of the traffic source during the lockdown, as a consequence of the strong restrictions on the population (Lamprecht et al., 2021). However, during the second lockdown, the diurnal profiles are more similar to the non-lockdown period than the first lockdown period. This could be explained by the weaker restrictions for the Autumn lockdown, resulting in more people going to work.



450

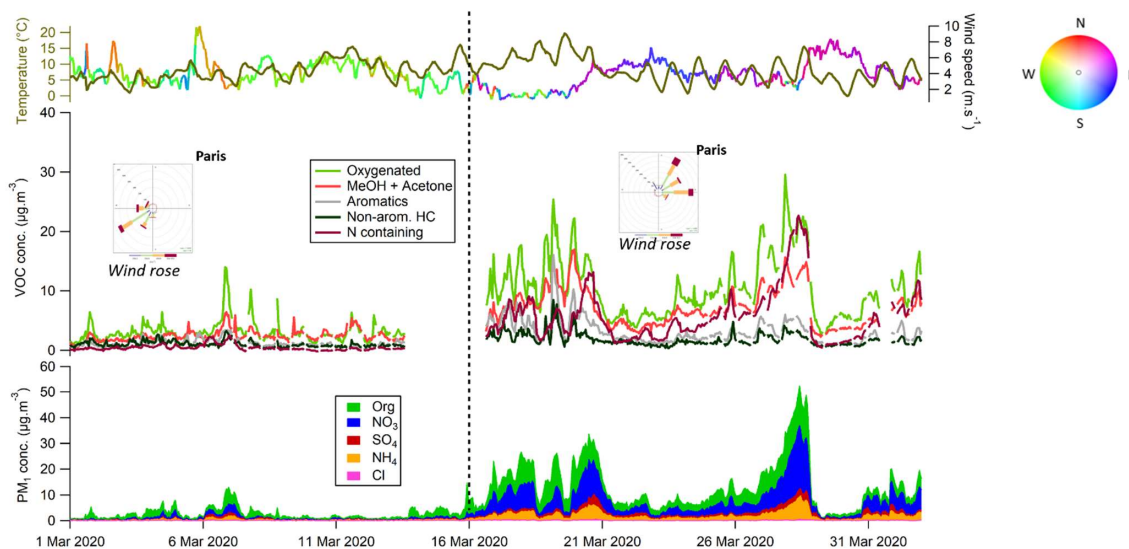
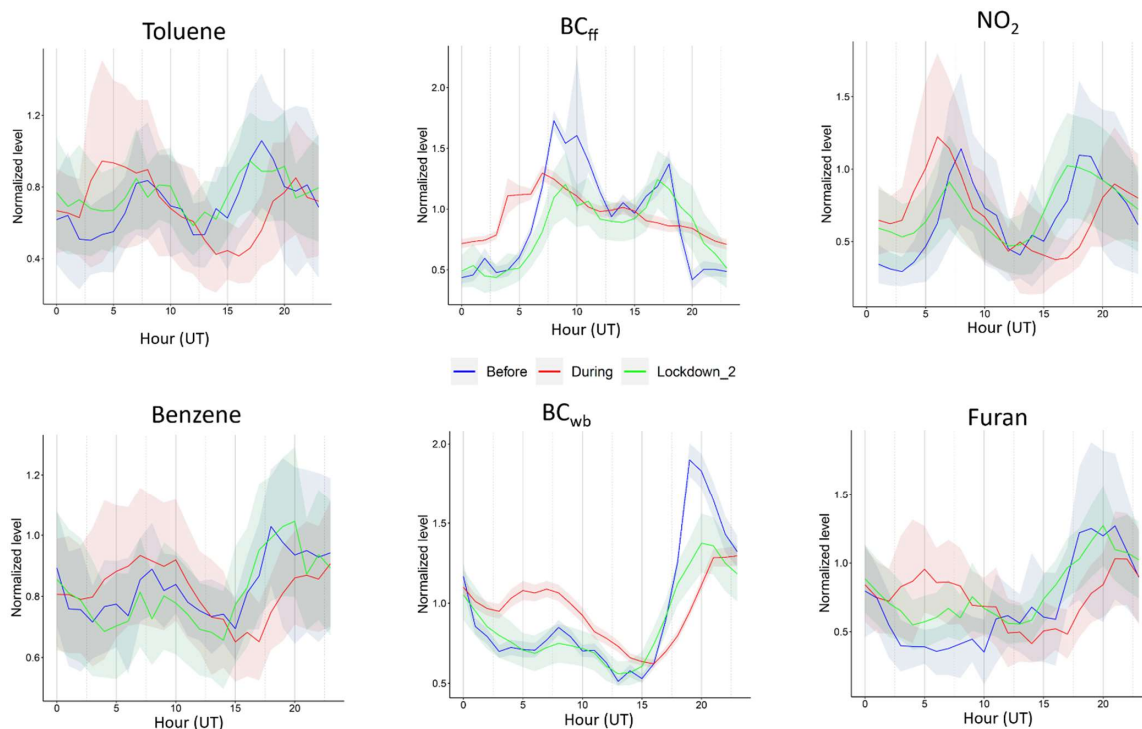


Figure 9: Time series of VOC, NR-PM1, temperature, wind speed and direction during the month of March 2020. The black dotted line marks the start of the Covid19-induced lockdown in France. Wind roses before (1–13 March) and during (16–31 March) are represented on the figure.

455 Figure 10 shows that, during the non-lockdown period, the diurnal profiles of benzene, furan, and the wood burning fraction of black carbon (BC_{wb}), are typical for the wood burning source (see Figure 8), and the additional small peak in the morning observed on the profile of benzene indicates that part of the emissions are from the traffic source. During the Spring lockdown, an additional peak appears in the morning for furan and BC_{wb} , and the morning peak of benzene is more pronounced. This could be due to people's presence at home during the day and their use of the fireplace in the morning, because it was still cold
460 at the end of March (mean temperature of 8.1°C). During the second lockdown, as observed for the traffic markers, the diurnal cycles of the wood burning markers resemble more those of the non-lockdown period than of the first lockdown, due to less strict regulations.

The investigation of the diurnal cycle's change during the Spring lockdown reflected the change in human activities on the pollutants in the atmosphere. The additional peak in the morning of the wood burning markers could have an impact on
465 secondary pollution formation, the study of which is beyond the scope of this paper.



470 **Figure 10: Diurnal cycles markers for the traffic source (toluene, BC_{ff}, NO₂) and for the wood burning source (benzene, BC_{wb}, furan) before (in blue, 1–13 March) and during (in red, 16–31 March) the Spring lockdown, and during the Autumn lockdown (in green, 30 October–15 December). The line represents the mean and the shaded area corresponds to 95% confidence interval. All diurnal cycles were normalised by the mean.**

4 Data availability

The dataset containing the volume mixing ratios (VMR, in ppb) for all measured mass-to-charge ratios are available on the IPSL Data Catalog (<https://data.ipsl.fr/catalog/srv/eng/catalog.search#/home>) under <https://doi.org/10.14768/f8c46735-e6c3-45e2-8f6f-26c6d67c4723> (Simon et al, 2022). For compounds that were quality assured by ACTRIS, flags are also given in this dataset, please refer to the associated read-me file. For the figures in the present paper, the data flagged “local contamination/local event” were not considered.

The dataset for the compounds that were quality assured by ACTRIS is also available on the EBAS database (<https://ebas.nilu.no/>); containing the VMR (in ppt), the uncertainties (precision and accuracy, in ppt) and flags, giving 480 indications on the state of the data. The flag references are the same for both datasets.



5 Conclusions

In this paper, we provide the first long-term VOC dataset obtained using PTR-MS measurements at a suburban site in Europe. This two-year dataset contains 31 mass-to-charge ratios (m/z) corresponding to 30+ compounds of interest for atmospheric chemistry research, identified thanks to additional PTR-ToF-MS measurements. The SIRTA station is part of ACTRIS, and
485 the data was carefully inspected following quality control and quality assurance procedures before being made available online. The analysis of the dataset conducted here enabled to highlight the specificities of VOCs in a suburban environment. Local sources such as traffic, wood burning and biogenic sources are marked on the compounds' diurnal cycle.

The VOC levels are driven here by their sources, meteorological conditions and air mass origin. This was investigated through the seasonal and diurnal variability. Our findings notably confirm the increase of aromatics and oxygenated compounds in
490 wintertime, due to additional wood burning source and boundary layer dynamics. On the other hand, oxygenated and biogenic VOCs were higher in summer due to increased temperature and solar radiation. Furthermore, a novel finding of the present study concerns the monoterpenes: their main source in a suburban area is supposedly biogenic, in this study their seasonal and diurnal variabilities brought out potential anthropogenic sources.

Investigation of the VOCs' geographic origins indicated that the more polluted air masses were the continental and North 1
495 (that both go through industrial areas and big cities, including Paris), and anticyclonic, highlighting the importance of local sources for short-life components like the VOCs. An interesting result here was the nitrogen-containing compounds, mainly m/z 46, brought to the station mostly by continental air masses, suggesting long-range transport. On an interannual basis, the increase or decrease of the VOC levels could be due to variability in the occurrence of oceanic vs continental air masses and not just the long-term tendency. For trend analysis of VOCs at SIRTA station, it is thus necessary to consider the air masses
500 and to do this trend analysis per cluster.

Finally, the investigation of the Covid19-induced lockdown in Spring emphasized the importance of meteorological conditions on the VOC levels. Diurnal cycles of compounds markers for anthropogenic sources before and during the lockdown showed a change in the compounds' behaviour, reflecting the change in human activities in this particular period.

This dataset will be used in a source apportionment study, in relation with organic aerosols, to better understand sources and
505 processes driving organic pollution. This dataset is available for modelling studies and can be used for emission inventories.

CRedit authorship statement

510 L. Simon: Conceptualization, Data curation, Formal analysis, Investigation, Visualization, Writing – original draft preparation, Writing – review & editing



- V. Gros: Conceptualization, Funding acquisition, Project administration, Resources, Supervision, Validation, Writing – review & editing
- J-E. Petit: Conceptualization, Funding acquisition, Project administration, Resources, Supervision, Validation, Writing – review & editing
- 515 F. Truong: Resources, Methodology, Software
- R. Sarda-Esteve: Resources
- C. Kalalian: Resources, Writing – review & editing
- C. Marchand: Conceptualization, Funding acquisition, Project administration, Supervision, Writing – review & editing
- 520 O. Favez: Conceptualization, Funding acquisition, Project administration, Resources, Supervision, Validation, Writing – review & editing

Competing interests

The authors declare that they have no conflict of interest.

Acknowledgements

- 525 The authors would like to acknowledge Sébastien Dusanter and Marina Jamar (IMT Nord Europe, France) for their help with the data quality evaluation, Stefan Reimann and Matthias Hill (EMPA, Switzerland) for ACTRIS quality control and Nicolas Pascal (Lille Univ., France), Christophe Boitel (LMD, France) and Sophie Bouffies-Cloch  (IPSL, France) for their help with the data submission to the ACTRIS Data Centre and IPSL databases. ACTRIS Data Centre and ACTRIS CiGas are acknowledged for their services and support in the QA, QC and data curation.
- 530 The authors also warmly thank Nicolas Bonnaire (LSCE, France) for providing NO_x and O₃ data and Dominique Baisnee (LSCE, France) for the help maintaining measurements during the lockdowns, as well as Melania Van Hove and Simone Kotthaus from SIRTIA-IPSL for providing the PAR and MHL data.

Financial support

- This work has benefited from the support of the research infrastructure ACTRIS-FR, registered on the Roadmap of the French Ministry of Research. This research has been supported by the H2020 ACTRIS-2 project (grant no 654109) and following
- 535 related projects. The authors also acknowledge financial support from CEA and CNRS.
- Leila Simon would like to acknowledge the DIM Qi² and Paris Ile-de-France region, as well as Ineris for her PhD's fellowship.



References

- 540 Ait-Helal, W., Borbon, A., Sauvage, S., de Gouw, J. A., Colomb, A., Gros, V., Freutel, F., Crippa, M., Afif, C., Baltensperger, U., Beekmann, M., Doussin, J.-F., Durand-Jolibois, R., Fronval, I., Grand, N., Leonardis, T., Lopez, M., Michoud, V., Miet, K., Perrier, S., Prévôt, A. S. H., Schneider, J., Siour, G., Zapf, P., and Locoge, N.: Volatile and intermediate volatility organic compounds in suburban Paris: variability, origin and importance for SOA formation, *Atmos. Chem. Phys.*, 14, 10439–10464, <https://doi.org/10.5194/acp-14-10439-2014>, 2014.
- 545 Aoki, N., Inomata, S., and Tanimoto, H.: Detection of C1–C5 alkyl nitrates by proton transfer reaction time-of-flight mass spectrometry, *International Journal of Mass Spectrometry*, 263, 12–21, <https://doi.org/10.1016/j.ijms.2006.11.018>, 2007.
- Barré, J., Petetin, H., Colette, A., Guevara, M., Peuch, V.-H., Rouil, L., Engelen, R., Inness, A., Flemming, J., Pérez García-Pando, C., Bowdalo, D., Meleux, F., Geels, C., Christensen, J. H., Gauss, M., Benedictow, A., Tsyro, S., Friese, E., Struzewska, J., Kaminski, J. W., Douros, J., Timmermans, R., Robertson, L., Adani, M., Jorba, O., Joly, M., and Kouznetsov, R.: Estimating lockdown induced European NO₂; changes, *Gases/Remote Sensing/Troposphere/Chemistry (chemical composition and reactions)*, <https://doi.org/10.5194/acp-2020-995>, 2020.
- 550 Baudic, A., Gros, V., Sauvage, S., Locoge, N., Sanchez, O., Sarda-Estève, R., Kalogridis, C., Petit, J.-E., Bonnaire, N., Baisnée, D., Favez, O., Albinet, A., Sciare, J., and Bonsang, B.: Seasonal variability and source apportionment of volatile organic compounds (VOCs) in the Paris megacity (France), *Atmos. Chem. Phys.*, 16, 11961–11989, <https://doi.org/10.5194/acp-16-11961-2016>, 2016.
- 555 Beekmann, M., Prévôt, A. S. H., Drewnick, F., Sciare, J., Pandis, S. N., Denier van der Gon, H. A. C., Crippa, M., Freutel, F., Poulain, L., Ghersi, V., Rodriguez, E., Beirle, S., Zotter, P., von der Weiden-Reinmüller, S.-L., Bressi, M., Fountoukis, C., Petetin, H., Szidat, S., Schneider, J., Rosso, A., El Haddad, I., Megaritis, A., Zhang, Q. J., Michoud, V., Slowik, J. G., Moukhtar, S., Kolmonen, P., Stohl, A., Eckhardt, S., Borbon, A., Gros, V., Marchand, N., Jaffrezo, J. L., Schwarzenboeck, A., 560 Colomb, A., Wiedensohler, A., Borrmann, S., Lawrence, M., Baklanov, A., and Baltensperger, U.: In situ, satellite measurement and model evidence on the dominant regional contribution to fine particulate matter levels in the Paris megacity, *Atmos. Chem. Phys.*, 15, 9577–9591, <https://doi.org/10.5194/acp-15-9577-2015>, 2015.
- Blake, R. S., Monks, P. S., and Ellis, A. M.: Proton-Transfer Reaction Mass Spectrometry, *Chem. Rev.*, 109, 861–896, <https://doi.org/10.1021/cr800364q>, 2009.
- 565 Borbon, A., Fontaine, H., Veillerot, M., Locoge, N., Galloo, J. C., and Guillermo, R.: An investigation into the traffic-related fraction of isoprene at an urban location, *Atmospheric Environment*, 35, 3749–3760, [https://doi.org/10.1016/S1352-2310\(01\)00170-4](https://doi.org/10.1016/S1352-2310(01)00170-4), 2001.
- Borbon, A., Gilman, J. B., Kuster, W. C., Grand, N., Chevallier, S., Colomb, A., Dolgorouky, C., Gros, V., Lopez, M., Sarda-Estève, R., Holloway, J., Stutz, J., Petetin, H., McKeen, S., Beekmann, M., Warneke, C., Parrish, D. D., and de Gouw, J. A.: 570 Emission ratios of anthropogenic volatile organic compounds in northern mid-latitude megacities: Observations versus emission inventories in Los Angeles and Paris: VOC EMISSION RATIOS IN MODERN MEGACITIES, *J. Geophys. Res. Atmos.*, 118, 2041–2057, <https://doi.org/10.1002/jgrd.50059>, 2013.
- Bruns, E. A., El Haddad, I., Slowik, J. G., Kilic, D., Klein, F., Baltensperger, U., and Prévôt, A. S. H.: Identification of significant precursor gases of secondary organic aerosols from residential wood combustion, *Sci Rep*, 6, 27881, <https://doi.org/10.1038/srep27881>, 2016.
- 575 Bruns, E. A., Slowik, J. G., El Haddad, I., Kilic, D., Klein, F., Dommen, J., Temime-Roussel, B., Marchand, N., Baltensperger, U., and Prévôt, A. S. H.: Characterization of gas-phase organics using proton transfer reaction time-of-flight mass



- spectrometry: fresh and aged residential wood combustion emissions, *Atmos. Chem. Phys.*, 17, 705–720, <https://doi.org/10.5194/acp-17-705-2017>, 2017.
- 580 Chen, Y., Takeuchi, M., Nah, T., Xu, L., Canagaratna, M. R., Stark, H., Baumann, K., Canonaco, F., Prévôt, A. S. H., Huey, L. G., Weber, R. J., and Ng, N. L.: Chemical characterization of secondary organic aerosol at a rural site in the southeastern US: insights from simultaneous high-resolution time-of-flight aerosol mass spectrometer (HR-ToF-AMS) and FIGAERO chemical ionization mass spectrometer (CIMS) measurements, *Atmos. Chem. Phys.*, 20, 8421–8440, <https://doi.org/10.5194/acp-20-8421-2020>, 2020.
- 585 Coggon, M. M., Lim, C. Y., Koss, A. R., Sekimoto, K., Yuan, B., Gilman, J. B., Hagan, D. H., Selimovic, V., Zarzana, K., Brown, S. S., Roberts, J. M., Müller, M., Yokelson, R., Wisthaler, A., Krechmer, J. E., Jimenez, J. L., Cappa, C., Kroll, J., de Gouw, J., and Warneke, C.: OH-chemistry of non-methane organic gases (NMOG) emitted from laboratory and ambient biomass burning smoke: evaluating the influence of furans and oxygenated aromatics on ozone and secondary NMOG formation, *Gases/Laboratory Studies/Troposphere/Chemistry (chemical composition and reactions)*, <https://doi.org/10.5194/acp-2019-516>, 2019.
- 590 Crippa, M., El Haddad, I., Slowik, J. G., DeCarlo, P. F., Mohr, C., Heringa, M. F., Chirico, R., Marchand, N., Sciare, J., Baltensperger, U., and Prévôt, A. S. H.: Identification of marine and continental aerosol sources in Paris using high resolution aerosol mass spectrometry: AEROSOL SOURCES IN PARIS USING HR-TOF-MS, *J. Geophys. Res. Atmos.*, 118, 1950–1963, <https://doi.org/10.1002/jgrd.50151>, 2013.
- 595 Daellenbach, K. R., Uzu, G., Jiang, J., Cassagnes, L.-E., Leni, Z., Vlachou, A., Stefenelli, G., Canonaco, F., Weber, S., Segers, A., Kuenen, J. J. P., Schaap, M., Favez, O., Albinet, A., Aksoyoglu, S., Dommen, J., Baltensperger, U., Geiser, M., El Haddad, I., Jaffrezo, J.-L., and Prévôt, A. S. H.: Sources of particulate-matter air pollution and its oxidative potential in Europe, *Nature*, 587, 414–419, <https://doi.org/10.1038/s41586-020-2902-8>, 2020.
- 600 Drinovec, L., Močnik, G., Zotter, P., Prévôt, A. S. H., Ruckstuhl, C., Coz, E., Rupakheti, M., Sciare, J., Müller, T., Wiedensohler, A., and Hansen, A. D. A.: The dual-spot Aethalometer: an improved measurement of aerosol black carbon with real-time loading compensation, *Atmos. Meas. Tech.*, 8, 1965–1979, <https://doi.org/10.5194/amt-8-1965-2015>, 2015.
- Duncianu, M., David, M., Kartigeyane, S., Cirtog, M., Doussin, J.-F., and Picquet-Varrault, B.: Measurement of alkyl and multifunctional organic nitrates by proton-transfer-reaction mass spectrometry, *Atmos. Meas. Tech.*, 10, 1445–1463, <https://doi.org/10.5194/amt-10-1445-2017>, 2017.
- 605 Favez, O., El Haddad, I., Piot, C., Boréave, A., Abidi, E., Marchand, N., Jaffrezo, J.-L., Besombes, J.-L., Personnaz, M.-B., Sciare, J., Wortham, H., George, C., and D’Anna, B.: Inter-comparison of source apportionment models for the estimation of wood burning aerosols during wintertime in an Alpine city (Grenoble, France), *Atmos. Chem. Phys.*, 10, 5295–5314, <https://doi.org/10.5194/acp-10-5295-2010>, 2010.
- 610 Gaimoz, C., Sauvage, S., Gros, V., Herrmann, F., Williams, J., Locoge, N., Perrussel, O., Bonsang, B., d’Argouges, O., Sarda-Estève, R., and Sciare, J.: Volatile organic compounds sources in Paris in spring 2007. Part II: source apportionment using positive matrix factorisation, *Environ. Chem.*, 8, 91, <https://doi.org/10.1071/EN10067>, 2011.
- Gkatzelis, G. I., Coggon, M. M., McDonald, B. C., Peischl, J., Gilman, J. B., Aikin, K. C., Robinson, M. A., Canonaco, F., Prevot, A. S. H., Trainer, M., and Warneke, C.: Observations Confirm that Volatile Chemical Products Are a Major Source of Petrochemical Emissions in U.S. Cities, *Environ. Sci. Technol.*, 55, 4332–4343, <https://doi.org/10.1021/acs.est.0c05471>, 2021.
- 615 de Gouw, J. and Warneke, C.: Measurements of volatile organic compounds in the earth’s atmosphere using proton-transfer-reaction mass spectrometry, *Mass Spectrom. Rev.*, 26, 223–257, <https://doi.org/10.1002/mas.20119>, 2007.



Gros, V., Gaimoz, C., Herrmann, F., Custer, T., Williams, J., Bonsang, B., Sauvage, S., Locoge, N., d'Argouges, O., Sarda-Estève, R., and Sciare, J.: Volatile organic compounds sources in Paris in spring 2007. Part I: qualitative analysis, *Environ. Chem.*, 8, 74–90, 2011.

620 Gueneron, M., Erickson, M. H., VanderSchelden, G. S., and Jobson, B. T.: PTR-MS fragmentation patterns of gasoline hydrocarbons, *International Journal of Mass Spectrometry*, 379, 97–109, <https://doi.org/10.1016/j.ijms.2015.01.001>, 2015.

Guenther, A., Hewitt, C. N., Erickson, D., Fall, R., Geron, C., Graedel, T., Harley, P., Klinger, L., Lerdau, M., McKay, W. A., Pierce, T., Scholes, B., Steinbrecher, R., Tallamraju, R., Taylor, J., and Zimmerman, P.: A global model of natural volatile organic compound emissions, *J. Geophys. Res.*, 100, 8873, <https://doi.org/10.1029/94JD02950>, 1995.

625 Haefelin, M., Barthès, L., Bock, O., Boitel, C., Bony, S., Bouniol, D., Chepfer, H., Chiriaco, M., Cuesta, J., Delanoë, J., Drobinski, P., Dufresne, J.-L., Flamant, C., Grall, M., Hodzic, A., Hourdin, F., Lapouge, F., Lemaître, Y., Mathieu, A., Morille, Y., Naud, C., Noël, V., O'Hirok, W., Pelon, J., Pietras, C., Protat, A., Romand, B., Scialom, G., and Vautard, R.: SIRTa, a ground-based atmospheric observatory for cloud and aerosol research, *Ann. Geophys.*, 23, 253–275, <https://doi.org/10.5194/angeo-23-253-2005>, 2005.

630 Hellén, H., Tykkä, T., and Hakola, H.: Importance of monoterpenes and isoprene in urban air in northern Europe, *Atmospheric Environment*, 59, 59–66, <https://doi.org/10.1016/j.atmosenv.2012.04.049>, 2012.

Joo, T., Rivera-Rios, J. C., Takeuchi, M., Alvarado, M. J., and Ng, N. L.: Secondary Organic Aerosol Formation from Reaction of 3-Methylfuran with Nitrate Radicals, *ACS Earth Space Chem.*, 3, 922–934, <https://doi.org/10.1021/acsearthspacechem.9b00068>, 2019.

635 Jordan, C., Fitz, E., Hagan, T., Sive, B., Frinak, E., Haase, K., Cottrell, L., Buckley, S., and Talbot, R.: Long-term study of VOCs measured with PTR-MS at a rural site in New Hampshire with urban influences, *Atmos. Chem. Phys.*, 21, 2009.

Kaltsonoudis, C., Kostenidou, E., Florou, K., Psichoudaki, M., and Pandis, S. N.: Temporal variability and sources of VOCs in urban areas of the eastern Mediterranean, *Atmos. Chem. Phys.*, 16, 14825–14842, <https://doi.org/10.5194/acp-16-14825-2016>, 2016.

640 Kammer, J., Décuq, C., Baisnée, D., Ciuraru, R., Lafouge, F., Buysse, P., Bsaibes, S., Henderson, B., Cristescu, S. M., Benabdallah, R., Chandra, V., Durand, B., Fanucci, O., Petit, J.-E., Truong, F., Bonnaire, N., Sarda-Estève, R., Gros, V., and Loubet, B.: Characterization of particulate and gaseous pollutants from a French dairy and sheep farm, *Science of The Total Environment*, 135598, <https://doi.org/10.1016/j.scitotenv.2019.135598>, 2019.

Kastler, J. and Ballschmiter, K.: Bifunctional alkyl nitrates - trace constituents of the atmosphere, *Fresenius' Journal of Analytical Chemistry*, 360, 812–816, <https://doi.org/10.1007/s002160050815>, 1998.

Knighton, W. B., Herndon, S. C., Shorter, J. H., Miake-Lye, R. C., Zahniser, M. S., Akiyama, K., Shimono, A., Kitasaka, K., Shimajiri, H., and Sugihara, K.: Laboratory Evaluation of an Aldehyde Scrubber System Specifically for the Detection of Acrolein, *Journal of the Air & Waste Management Association*, 57, 1370–1378, <https://doi.org/10.3155/1047-3289.57.11.1370>, 2007.

650 Kroll, J. H., Ng, N. L., Murphy, S. M., Flagan, R. C., and Seinfeld, J. H.: Secondary Organic Aerosol Formation from Isoprene Photooxidation, *Environ. Sci. Technol.*, 40, 1869–1877, <https://doi.org/10.1021/es0524301>, 2006.



- Lamprecht, C., Graus, M., Striednig, M., Stichaner, M., and Karl, T.: Decoupling of urban CO₂; and air pollutant emission reductions during the European SARS-CoV-2 lockdown, *Atmos. Chem. Phys.*, 21, 3091–3102, <https://doi.org/10.5194/acp-21-3091-2021>, 2021.
- 655 Languille, B., Gros, V., Petit, J.-E., Honoré, C., Baudic, A., Perrussel, O., Foret, G., Michoud, V., Truong, F., Bonnaire, N., Sarda-Estève, R., Delmotte, M., Feron, A., Maisonneuve, F., Gaimoz, C., Formenti, P., Kotthaus, S., Haefelin, M., and Favez, O.: Wood burning: A major source of Volatile Organic Compounds during wintertime in the Paris region, *Science of The Total Environment*, 711, 135055, <https://doi.org/10.1016/j.scitotenv.2019.135055>, 2020.
- Larsen, B. R., Bella, D. D., Glasius, M., Winterhalter, R., Jensen, N. R., and Hjorth, J.: Gas-Phase OH Oxidation of
660 Monoterpenes: Gaseous and Particulate Products, 46, 2000.
- Lefohn, A. S., Malley, C. S., Smith, L., Wells, B., Hazucha, M., Simon, H., Naik, V., Mills, G., Schultz, M. G., Paoletti, E., De Marco, A., Xu, X., Zhang, L., Wang, T., Neufeld, H. S., Musselman, R. C., Tarasick, D., Brauer, M., Feng, Z., Tang, H., Kobayashi, K., Sicard, P., Solberg, S., and Gerosa, G.: Tropospheric ozone assessment report: Global ozone metrics for climate change, human health, and crop/ecosystem research, *Elementa: Science of the Anthropocene*, 6, 27,
665 <https://doi.org/10.1525/elementa.279>, 2018.
- Lindinger, W., Jordan, A., and Hansel, A.: Proton-transfer-reaction mass spectrometry (PTR-MS): on-line monitoring of volatile organic compounds at pptv levels, *Chem. Soc. Rev.*, 27, 347, <https://doi.org/10.1039/a827347z>, 1998.
- Mahilang, M., Deb, M. K., and Pervez, S.: Biogenic secondary organic aerosols: A review on formation mechanism, analytical challenges and environmental impacts, *Chemosphere*, 262, 127771, <https://doi.org/10.1016/j.chemosphere.2020.127771>,
670 2021.
- Mayorga, R. J., Zhao, Z., and Zhang, H.: Formation of secondary organic aerosol from nitrate radical oxidation of phenolic VOCs: Implications for nitration mechanisms and brown carbon formation, *Atmospheric Environment*, 244, 117910, <https://doi.org/10.1016/j.atmosenv.2020.117910>, 2021.
- McDonald, B. C., de Gouw, J. A., Gilman, J. B., Jathar, S. H., Akherati, A., Cappa, C. D., Jimenez, J. L., Lee-Taylor, J., Hayes, P. L., McKeen, S. A., Cui, Y. Y., Kim, S.-W., Gentner, D. R., Isaacman-VanWertz, G., Goldstein, A. H., Harley, R. A., Frost, G. J., Roberts, J. M., Ryerson, T. B., and Trainer, M.: Volatile chemical products emerging as largest petrochemical source of urban organic emissions, *Science*, 359, 760–764, <https://doi.org/10.1126/science.aag0524>, 2018.
- Müller, M., Graus, M., Wisthaler, A., Hansel, A., Metzger, A., Dommen, J., and Baltensperger, U.: Analysis of high mass resolution PTR-TOF mass spectra from 1,3,5-trimethylbenzene (TMB) environmental chamber experiments, *Atmos. Chem. Phys.*, 12, 829–843, <https://doi.org/10.5194/acp-12-829-2012>, 2012.
680
- Ng, N. L., Herndon, S. C., Trimborn, A., Canagaratna, M. R., Croteau, P. L., Onasch, T. B., Sueper, D., Worsnop, D. R., Zhang, Q., Sun, Y. L., and Jayne, J. T.: An Aerosol Chemical Speciation Monitor (ACSM) for Routine Monitoring of the Composition and Mass Concentrations of Ambient Aerosol, *Aerosol Science and Technology*, 45, 780–794, <https://doi.org/10.1080/02786826.2011.560211>, 2011.
- 685 Panopoulou, A., Liakakou, E., Sauvage S., Gros, V., Locoge N., Stavroulas, I., Bonsang, B., Gerasopoulos, E., Mihalopoulos, N.: Yearlong measurements of monoterpenes and isoprene in a Mediterranean city (Athens): Natural vs anthropogenic origin, *Atmospheric Environment*, 12, <https://doi.org/10.1016/j.atmosenv.2020.117803> 2020.
- Petit, J.-E., Favez, O., Sciare, J., Crenn, V., Sarda-Estève, R., Bonnaire, N., Močnik, G., Dupont, J.-C., Haefelin, M., and
690 Leoz-Garziandia, E.: Two years of near real-time chemical composition of submicron aerosols in the region of Paris using an



- Aerosol Chemical Speciation Monitor (ACSM) and a multi-wavelength Aethalometer, *Atmos. Chem. Phys.*, 15, 2985–3005, <https://doi.org/10.5194/acp-15-2985-2015>, 2015.
- Petit, J.-E., Favez, O., Albinet, A., and Canonaco, F.: A user-friendly tool for comprehensive evaluation of the geographical origins of atmospheric pollution: Wind and trajectory analyses, *Environmental Modelling & Software*, 88, 183–187, <https://doi.org/10.1016/j.envsoft.2016.11.022>, 2017.
- Petit, J.-E., Dupont, J.-C., Favez, O., Gros, V., Zhang, Y., Sciare, J., Simon, L., Truong, F., Bonnaire, N., Amodeo, T., Vautard, R., and Haefelin, M.: Response of atmospheric composition to COVID-19 lockdown measures during spring in the Paris region (France), *Atmos. Chem. Phys.*, 21, 17167–17183, <https://doi.org/10.5194/acp-21-17167-2021>, 2021.
- Sandradewi, J., Prévôt, A. S. H., Szidat, S., Perron, N., Alfarra, M. R., Lanz, V. A., Weingartner, E., and Baltensperger, U.: Using Aerosol Light Absorption Measurements for the Quantitative Determination of Wood Burning and Traffic Emission Contributions to Particulate Matter, *Environ. Sci. Technol.*, 42, 3316–3323, <https://doi.org/10.1021/es702253m>, 2008.
- Sciare, J., d’Argouges, O., Sarda-Estève, R., Gaimoz, C., Dolgorouky, C., Bonnaire, N., Favez, O., Bonsang, B., and Gros, V.: Large contribution of water-insoluble secondary organic aerosols in the region of Paris (France) during wintertime: WINTERTIME WATER-INSOLUBLE SOA, *J. Geophys. Res.*, 116, n/a-n/a, <https://doi.org/10.1029/2011JD015756>, 2011.
- Seinfeld, J. H. and Pandis, S. N.: *Atmospheric chemistry and physics: from air pollution to climate change*, 2nd ed., J. Wiley, Hoboken, N.J., 1203 pp., 2006.
- Simon, L., Gros V., Truong F., Sarda-Estève R., Kalalian, C., PTR-MS measurements in 2020-2021, IPSL Data Catalog [dataset], <https://doi.org/10.14768/f8c46735-e6c3-45e2-8f6f-26c6d67c4723>, 2022.
- Steinbrecher, R., Smiatek, G., Köble, R., Seufert, G., Theloke, J., Hauff, K., Ciccioli, P., Vautard, R., and Curci, G.: Intra- and inter-annual variability of VOC emissions from natural and semi-natural vegetation in Europe and neighbouring countries, *Atmospheric Environment*, 43, 1380–1391, <https://doi.org/10.1016/j.atmosenv.2008.09.072>, 2009.
- Taipale, R., Ruuskanen, T. M., Rinne, J., Kajos, M. K., Hakola, H., Pohja, T., and Kulmala, M.: Technical Note: Quantitative long-term measurements of VOC concentrations by PTR-MS – measurement, calibration, and volume mixing ratio calculation methods, *Atmos. Chem. Phys.*, 18, 2008.
- Verreyken, B., Amelynck, C., Schoon, N., Müller, J.-F., Brioude, J., Kumpp, N., Hermans, C., Metzger, J.-M., and Stavrakou, T.: Measurement report: Source apportionment of volatile organic compounds at the remote high-altitude Maïdo observatory, *Gases/Field Measurements/Troposphere/Chemistry (chemical composition and reactions)*, <https://doi.org/10.5194/acp-2021-124>, 2021.
- Wagner, P. and Kuttler, W.: Biogenic and anthropogenic isoprene in the near-surface urban atmosphere — A case study in Essen, Germany, *Science of The Total Environment*, 475, 104–115, <https://doi.org/10.1016/j.scitotenv.2013.12.026>, 2014.
- Yu, J., Iii, D. R. C., Griffin, R. J., Flagan, R. C., and Seinfeld, J. H.: Gas-Phase Ozone Oxidation of Monoterpenes: Gaseous and Particulate Products, 52, 1999.
- Yuan, B., Coggon, M. M., Koss, A. R., Warneke, C., Eilerman, S., Peischl, J., Aikin, K. C., Ryerson, T. B., and de Gouw, J. A.: Emissions of volatile organic compounds (VOCs) from concentrated animal feeding operations (CAFOs): chemical compositions and separation of sources, *Atmos. Chem. Phys.*, 17, 4945–4956, <https://doi.org/10.5194/acp-17-4945-2017>, 2017a.



Yuan, B., Koss, A. R., Warneke, C., Coggon, M., and Sekimoto, K.: Proton-Transfer-Reaction Mass Spectrometry: Applications in Atmospheric Sciences, *Chem. Rev.*, 43, 2017b.

730 Zhang, Y., Favez, O., Petit, J.-E., Canonaco, F., Truong, F., Bonnaire, N., Crenn, V., Amodeo, T., Prévôt, A. S. H., Sciare, J., Gros, V., and Albinet, A.: Six-year source apportionment of submicron organic aerosols from near-continuous highly time-resolved measurements at SIRTÀ (Paris area, France), *Atmos. Chem. Phys.*, 19, 14755–14776, <https://doi.org/10.5194/acp-19-14755-2019>, 2019.